ILASS 2008
Sep. 8-10, 2008, Como Lake, Italy

Paper ID ILASS08-2-7

SIMULATION OF TWO-PHASE FLOWS IN INJECTORS WITH THE CFD CODE EOLE

R. Marcer°, C. Dassibat°, B. Argueyrolles*

(°) PRINCIPIA R. & D., AREVA Group, Zone Athélia 1 – 13705 La Ciotat – France
(*) RENAULT Powertrain Division, 1 Allée Cornuel - 91510 Lardy - France

ABSTRACT
In high pressure diesel injection processes, the flow is led by mass transfer mechanisms. Indeed, cavitation of the flow occurs due to the drop of the static pressure locally induced by geometrical constraints: in the needle seat and at the hole inlets. The presence of unsteady cavitation which depends on characteristics of the holes and of the needle, strongly affects the instantaneous values of the flow rate, the injection velocity, the diesel fuel hydraulic area and the injection angle.
A numerical code (EOLE) for the simulation of cavitating diesel flows has been developed. It is based on a multiphase Navier-Stokes model using a VOF interface tracking method able to calculate the cavitation evolution within Diesel injectors, taking into account the mass transfer process at the liquid-vapour interfaces.
The needle motion is computed with a grid deformation technique based on a sliding nodes method. This method allows getting very well conditioned meshes even when the opening of the needle is very small and so the cells of the mesh very squeezed.
The model has been validated on the basis of comparisons with measurements on different kinds of injector. The paper shows some further validations of the model especially on axi-symmetrical and unsymmetrical one-hole injectors, as well as on multi-hole injectors, considering a moving needle.

INTRODUCTION

The advantages of the very high pressure injection (> 160 MPa) provided by common rail injectors do not need to be proven any more. The race for the highest injection pressure does not seem to be close to the end, the main reason beeing the allowance to use always smaller holes in order to limit the pollutants at low load without penalty on the performances at full load. This leads, taking into account the reduction of hole size, to use strongly hydro-eroded convergent conical holes, a priori free of cavitation, but this can in parallel give rise to risks of coking. For that reason, one has to find compromises and to come back to low cavitating holes because one knows that the presence of cavitation limits the risks of coking. Furthermore, some experiments, for example Busch [1], have shown that cavitation may appear in the needle seat area during the needle opening or closing phase. So, the flow calculation at the nozzle hole exit (temporal profiles of the flow rate, of the velocity, of the spray micro-angle) which influences directly the quality of the calculations of spray penetration and combustion has necessary to take into account the two-phase flow aspects which may occur into the nozzle. These calculations necessitate to be all the more precise as the hole geometries, which may be in use in the near future, should belong rather to a transition domain between non cavitating and strongly cavitating flow.

Generally speaking, the cavitation phenomena which may occur into nozzle holes are complex phenomena which depend on a great number of geometrical parameters (hole conicity, hole inlet radii of curvature, hole orientation, roughness…) and on the flow operating conditions (sac pressure, back pressure, maximum needle lift and needle lift velocity profile).

Visualisation and measurements in the cavitating flows

The cavitation appearance in nozzle holes has been the topic of many experimental studies. Some of these studies were done on enlarged nozzles keeping a dynamic similarity on the Reynolds number and on the cavitation number but some aspects such as the ratio between the convection time and the life duration of the cavitation bubbles or the ratio between their diameter and the hole diameter cannot in principle be maintained [2]. We will focus in the following more particularly on experiments close to real size, being conscious also that very useful results can be obtained on enlarged nozzles [3].

The real size experiments were at first performed on orifices or one hole injectors for stationary boundary conditions. Chaves [2] for example, observes the formation of cavitation sheets which are shedded as cavitation pockets or bubbles. Direct measurements of injection velocity (locally close to Bernoulli velocity) and of the frequency of bubble emission through the exit are available in his study. Winklhofer [4] has characterized the flow into throttles of various conicities at fixed upstream pressure (10 MPa) and for variable back pressures. The pressure field obtained through the use of micro-interferometry is described and also the radial velocity profiles at various abscissa. These profiles are obtained from the temporal shift of the Laser Induced Fluorescence signal during the crossing of a laser beam through the hole radial direction.

Collicott [5] has also worked on throttles for pressures as high as 200 MPa. For the highest pressures (Pinj> 87 MPa), the surface conditions seam to play a very important role. Walther

[6] has worked on transparent one-hole axial injectors with various inlet radii of curvature. Correlations were obtained between spray break-up and cavitation for various cavitation numbers, for the same density of the downstream medium. Radial mean velocity profiles were obtained by PIV with fluorescent tracers in various cross-sections orthogonally to the hole axis. Thereafter the same methodology was applied on three hole transparent nozzles for two needle lifts.

Experiments on multi-hole injectors with partially or totally transparent nozzles were done by Arcoumanis [8], Busch [1] and Miranda [9]. Arcoumanis [8] used a nozzle equipped with a transparent insert at an injection pressure equal to 120 MPa. He shows for stationary operating conditions (fixed needle) the appearance of cavitation sheets, which beyond the recirculation zone at the hole inlet are shedded as cavitation bubbles. He shows also that cavitation strings may appear in a stochastic way, mainly at high needle lift, between adjacent holes, or initiate on the needle tip (especially for VCO nozzles at low lift [3]). Then these cavitation strings penetrate into the holes and interact with the lying "geometrical" cavitation. The presence of such cavitation strings was confirmed by Busch [1] in a transparent 6 hole injector operated at 60 MPa with a moving needle. These strings do not appear any more if the nozzle has only one flowing skew hole. Busch shows clearly the appearance of cavitation at the needle seat for low lifts, this cavitation may, after convection, ease the onset of cavitation in the hole itself. He confirms the importance of the surface conditions for high pressures (120 MPa). Finally several authors [1], [3], [9] observe a swirling flow around the cavitation sheets at low needle lift.

Saliba [10] observed also the evolution of cavitation for a transparent one-hole axial injector with injection pressures as high as 70 MPa and a moving needle. Correlations were done between the percentage of needle lift aperture, the percentage of the longitudinal hole cross-section occupied by cavitation, some spray characteristics, and this for various hole geometries.

By another way, the cavitation spread depends mainly on the cavitation number and not on the Reynolds number, Soteriou [12], Arcoumanis [8]. This is the same for the critical cavitation number but some experiments of Payri [13], let think that a dependency exists for low injection pressures (Pinj<50 MPa) (figure 8 of [13] plotted as Kcrit= $(\Delta P/Pch)crit = f(\Delta P)$).

When the sac pressure evolves in a transient way, the shape of cavitation does not appear as a quasi-steady process. The cavitation spread into the hole depends on the imposed upwind pressure gradient [14]. More generally, the cavitation spread depends on the sense of the imposed upwind and/or downwind pressure gradient.

Links with the spray break-up

Various authors have considered the links between cavitation and spray break-up [3],[6],[7]. Walther [6] shows that the appearance of cavitation at the hole inlet is sufficient for an increase of the spray break-up at the hole exit, which induces a larger spray angle. This influence of cavitation, at a distance, seems to be due to some extra turbulence generated at the hole inlet and thereafter convected [3]. But the increase of spray angle levels off when the Reynolds number further increases, as long as cavitation does not arrive at the hole exit [6]. When the cavitation sheet arrives at the hole exit, the injection velocity is notably reinforced due to the reduced liquid flow area and the liquid does not develop any boundary layer along the cavitation sheet, which increases still further the liquid-gas velocity gradient at the hole exit. The role of the implosion of cavitation bubbles in relation to the spray break-up is still unclear (extra turbulence, flow rate modulation…). The experiments of Badock [7] however seem to show that there is no direct correlation between the implosion of cavitation bubbles and the intensity of spray break-up.

Numerical approaches

Various methods can be found in the literature for calculating cavitation phenomena in injector flows : mixture model using a barotropic equation artificially smoothed [17], [18], [19], or based on the Rayleigh-Plesset (R-P) equation [20], two-fluid formulation of the conservation laws with use of the R-P equation for the calculation of the inter-phase transfer source terms [15], [21] (code Fire), [22] (code Fluent), eulerian formulation allowing to treat the vapour phase as a continuous vapour cloud with no-slip velocity between phases [17-20], lagrangian formulation where the vapour is treated as discrete vapour bubbles whose trajectories are calculated on a eulerian frame of reference [15].

Other codes such as Eole use a tracking interface methodology. This code has been described by Marcer et al. [23], [24] and will be briefly reminded in the following. We chose this methodology mainly due to the experimental evidence that cavitation appears as sheets for real size geometries, at least at the entrance of nozzle holes.

Validations of the codes for injection applications can be found in [25],[26].

However it has to be noted that all these numerical methodologies can only handle deterministic events and cannot take into account stochastic phenomena such as "string cavitation" observed for example by Arcoumanis et al. [8].

THE NUMERICAL MODEL

Generally speaking, in the code Eole, a modified VOF method is used to simulate both the kinematic motion of the liquid-vapour interface and the mass-transfer thermodynamical process from an added source term in the VOF conservation equation. In this method, the specific liquid and vapour density of each phase are taken into account.
The liquid phase may be compressible due to the high velocity and pressure gradients existing in the nozzle cavitating flow. The density variation being related to dynamic but not to thermal effect, an equation of state is introduced, where the local density is a function of the local pressure. The molecular viscosity depends also on the pressure, considering isothermal flow conditions. The turbulent nature of the flow is taken into account through a k-ε model.

Numerical method

The flow solver is based on an original pseudo-unsteady system [27]. The pseudo-compressibility method used in Eole differs from the classical method of Chorin. It is based on the idea of searching for pseudo-unsteady systems which, in the inviscid case, approach the exact unsteady compressible Euler equations as much as possible. For this purpose, pseudo-time derivative terms associated with a time-like variable $\tilde{\tau}$ called pseudo-time are introduced. The pseudo-time derivative term is constructed by replacing the true density by a pseudo-

density, and the pressure is calculated as a given function, called pseudo equation of state, of this pseudo-density.

$$p^{n+1} = f(\tilde{\rho}^{n+1}) \qquad (1)$$

Considering a fully implicit second order scheme for the time discretization and the semi-discretized equations at the time level n+1, the curvilinear system is written:

$$\frac{1}{J}\frac{\partial \tilde{W}^{n+1}}{\partial \tau} + \frac{1}{J}\frac{3W^{n+1} - 4W^{n} + W^{n-1}}{2\Delta t} + \left(\frac{\partial F}{\partial \xi}\right)^{n+1} + \left(\frac{\partial G}{\partial \eta}\right)^{n+1} + \left(\frac{\partial H}{\partial \chi}\right)^{n+1} = \frac{T}{J}^{n+1} \qquad (2)$$

with the dependent variables vector $\tilde{W} = \begin{pmatrix} \tilde{\rho} \\ \tilde{\rho}u \\ \tilde{\rho}v \\ \tilde{\rho}w \end{pmatrix}$,

and *F,G,H* the flux terms including convective, pressure, molecular and turbulent diffusion. The *T* term is the surface tension force and *J* is the jacobian matrix of the coordinates transformation.

The code uses a finite volume method. The discretization in space is fully centered and artificial viscosity terms of fourth order are added to damp the numerical oscillations.

Integration in pseudo-time makes use of an explicit five stage Runge-Kutta scheme. An implicit residual smoothing operator is also applied following each stage of the Runge-Kutta scheme to improve stability.

The interest of local pseudo-time stepping is to greatly increase the convergence rate. This method is then particularly convenient to deal with multi-phase flows having phases with high density ratios.

The code runs on multi-processors machines, in MPI/OMP parallel mode.

Deforming meshes

The equations are discretized on curvilinear moving and deforming meshes.

The original deforming mesh method used in the code is based on a no-slip nodes technique. The algorithm allows to calculate a new mesh at each time step, according to the needle lift law. This intermediate mesh is interpolated between two opposite meshes corresponding respectively to the fully closed and fully open positions of the needle, both having the same topology.

In this method, the mesh nodes situated on the needle remain fixed during its motion (figure 1). Due to topology constraints, distorted cells might be issued when the needle approachs the opposite fixed wall. For an injector, this method does not give correct meshes when the opening of the needle is less than 20µm.

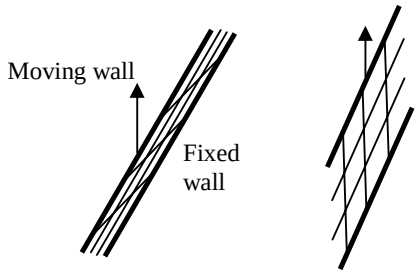

Figure 1: Distorted cells with the no-slip nodes method

The need to get accurate results for low needle openings led us to develop a new methodology for the mesh deformation where the grid nodes are allowed to slide along the moving wall (needle). In this case, the grid lines are imposed perpendicular to the needle so that the mesh remains well-conditioned as the needle is moving (figure 2). For an injector, meshes with very low needle openings (on the order of 2 µm only) can be built with this sliding nodes method.

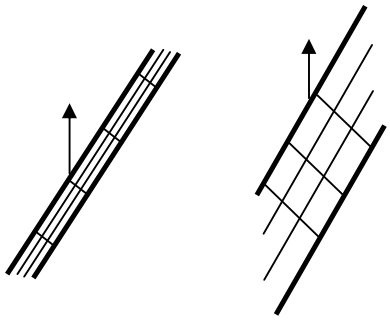

Figure 2: Well conditioned deformation with the sliding nodes method

The interface VOF model

The numerical simulation of two-phase flows with phases separated by sharp interfaces, such as sheet cavitation (as opposed to cavitation bubble flows), requires the simultaneous solution of the Navier-Stokes equations in the two fluids and of the kinematic displacement of the interfaces. Among the different kinds of interface tracking methods, the VOF model is one of the most efficient because of its ability to represent complex deformations of interfaces including break-up.

The VOF method introduces a discrete function *C* whose value (located between 0 and 1) in each cell is the fraction of the cell occupied by the liquid. The fraction *1-C* of the cell volume is then occupied by vapour (cavitation).

The transport of the *C* fraction, i.e the motion of the interface in the fixed mesh, can be ensured by a lagrangian method [28] or a classical eulerian method where a conservation equation of C is written :

$$\frac{\partial C}{\partial t} + div\left[\rho\left(\vec{U} - \vec{W}\right)\right]C = O \qquad (3)$$

where $\vec{U}$ is the liquid velocity at the interface and $\vec{W}$ is the grid velocity.

3

The cavitation model

The onset of cavitation, i.e the passage of a non-cavitating one-phase flow to a two-phase cavitating flow, is carried out when the pressure in the liquid flow reaches locally a critical threshold corresponding to the vapour pressure of the liquid phase. In this condition, the cavitation is initialized in cells of the mesh which fulfill this vaporization criterion.

Then, the motion of the interface is achieved by the kinematic part of the VOF model, with a velocity equal to the normal velocity of the liquid, coupled with a thermodynamical part characterizing the mass transfer process (vaporization and condensation).

Two cavitation models, developed by Principia, have been implemented in EOLE to simulate the mass transfer processes through liquid-vapour interfaces [23],[24].

In the KMT1-VOF model (Kinematics and Mass Transfer VOF model) the mass transfer is taken into account through a semi-empirical cavitation criterion. At each time step, an instantaneous mass transfer is imposed into liquid cells of the mesh having a pressure lower than the vapour pressure. The position of the liquid-vapour interface computed by the VOF interface (representative of the purely kinematic part of the cavitating flow) is then corrected in order to take into account thermodynamical effects. So the "kinematic" VOF field is modified in such a way that the interface is constrained to fit the vapour pressure isobar and therefore the pressure of the liquid phase is higher than the vapour pressure. In this model the mass transfer source term C_t is a function of the pressure gradient field.

The second model (KMT2-VOF model) is based on the hypothesis that the thermal diffusion effects are negligible inside the two-phase domain. In this case, we can show that the vapour or liquid source term C_t can be written as:

$$C_t = \frac{dC}{dt} = -\frac{1}{A}\left(\frac{\partial P}{\partial t} + B\frac{dP}{dt} + \rho\frac{dE_C}{dt}\right) \quad (4)$$

where A and B are functions of the liquid volume fraction *C*, the pressure, the liquid and vapour densities and the velocity of sound in the two phase zone, and E_C is the mean specific kinetic energy. Details of the model can be found in [24].

Once the source term C_t is computed, it is integrated in the VOF model in order to take into account the thermodynamical effects occurring during the vaporization and the condensation of the fluid. The new equation for the VOF becomes

$$\frac{\partial C}{\partial t} + div\left[\rho\left(\vec{U} - \vec{W}\right)\right]C = C_t \quad (5)$$

where C_t is the mass transfer term.

NUMERICAL RESULTS

Examples of numerical applications are given hereafter. Some of them are compared with measurements of cavitation patterns and velocity fields of the two-phase flow.

Axisymmetrical one hole injectors

The first example is issued from the PhD work of J. Walther at Technische Universität Darmstadt [6]. This author has used in particular transparent nozzles with one axial hole. The needle lift is fixed at maximum lift. One of his geometries (D200) has a rather straight entrance allowing the appearance of cavitation. Tests have been carried out for various cavitation numbers and for a given ΔP at the same density of the downstream medium, in order to see directly the effect of cavitation on the spray break-up. PIV measurements of the local velocities have been performed with Nd-Yag laser beams on fluorescent tracers flowing with the liquid. The index of the liquid is adapted to the plexiglas of the transparent nozzle and the measurement plane is selected through the depth of field of a long distance microscope. For each operating condition, the radial profiles of the axial velocities have been acquired at various distances from the hole inlet. Pictures obtained by shadowgraphy complete these measurements. Thereafter, the same methodology was applied to three hole nozzles for two needle lifts. These measurements (PIV and cavitation pictures) are particularly interesting for a fine evaluation of any two-phase flow code.

The geometry D200 has been considered in our calculations. The hole length is 1mm and the hole diameter 205 µm. The radius of curvature Rc at the hole entrance is not specified but should not exceed 10 µm. This value was used in the following calculations. For this geometry, the cavitation appears at a rather large cavitation number (=50), but this is probably due to the flow arriving axially into the hole and to the smooth plexiglas walls. Even a very small inlet radius of curvature tends to inhibit the recirculation of the flow, where the onset of cavitation occurs

The first operating condition that we considered is 10 MPa into 0.1 MPa. In this case, the cavitation has a spread limited to the hole entrance but has already an indirect effect on the spray break-up and so on the microscopic spray angle [6].
The calculations were performed here without the needle in place, but this should not have too much effect on the results. Some tests were done concerning the correct number of cells lying in the radial direction of the hole. After these tests, 20 cells along the radius appeared sufficient.

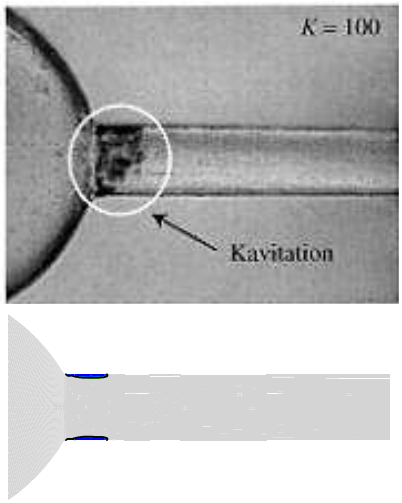

Figure 3: Cavitation pattern - Rc=10 µm – 10 MPa /0.1 MPa comparison EOLE/measurements [6].

4

The results are presented in a vertical plane cut passing through the hole axis. The length of the cavitation sheet and its lateral spread are correctly reproduced by the model (figure 3).
In the experimental results of figure 4, all the PIV results have been gathered and plotted in a vertical plane by J. Walther, with a scale expressed as a percentage of the Bernoulli velocity. Our numerical results are now compared in the same plane, with the same scale and show a similar increase of the velocity, particularly in the contracted liquid section near the hole entrance due to the presence of the cavitation sheet (figure 4). This increase appears preferably along the cavitation zones.

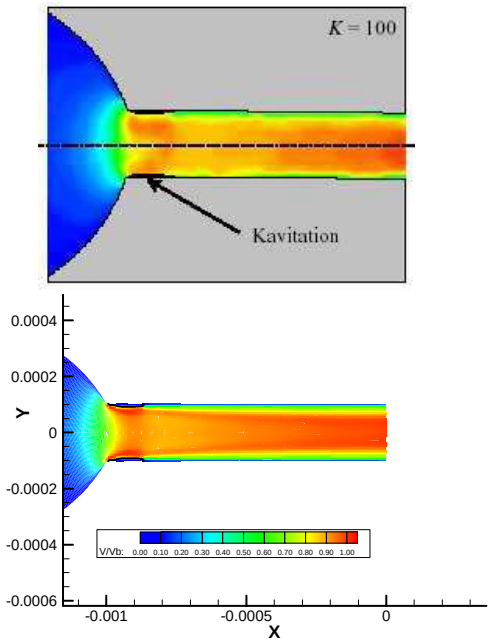

Figure 4: Velocity field / Bernoulli velocity - Rc=10 µm 10 MPa / 0.1 MPa - comparison EOLE/PIV measurements [6].

A comparison is done in figure 5 on the axial velocity profile at 350 µm, i.e downstream the cavitation zones. The level of the calculated velocity (0.9VBernoulli) is correctly reproduced on the axis, but the wake effect downstream the cavitation sheets is a little bit more marked along the walls (see also figure 4).

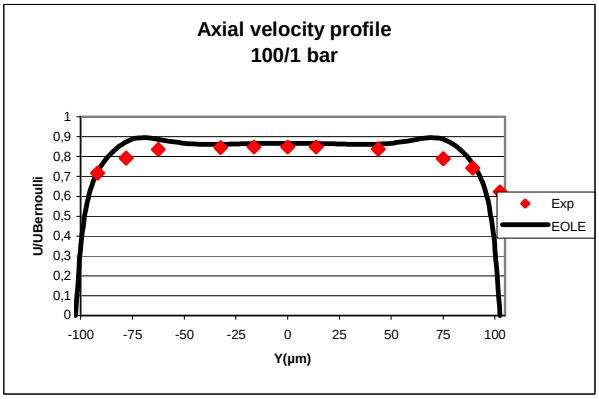

Figure 5: Comparison EOLE/PIV measurements [6] of the radial velocity profile in a section of the hole located at 350 µm from the hole inlet- Rc=10 µm – 10 Mpa / 0.1 MPa

The second operating condition that we considered is 15 MPa into 0.1 MPa. In this case, the cavitation spreads experimentally until the hole outlet (supercavitation).
The calculation retrieves this result and the velocity field is globally compared in figures 6 and 7.

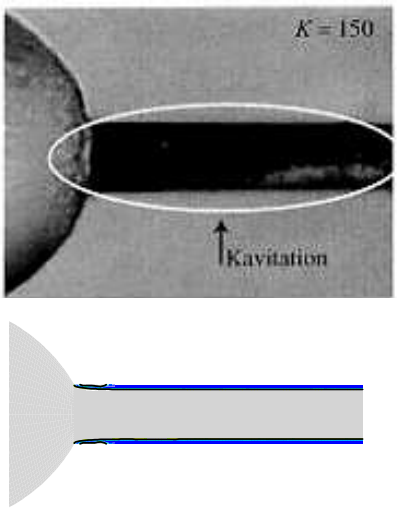

Figure 6: Cavitation pattern – Rc=10 µm – 15 MPa / 0.1 MPa comparison EOLE/measurements [6]

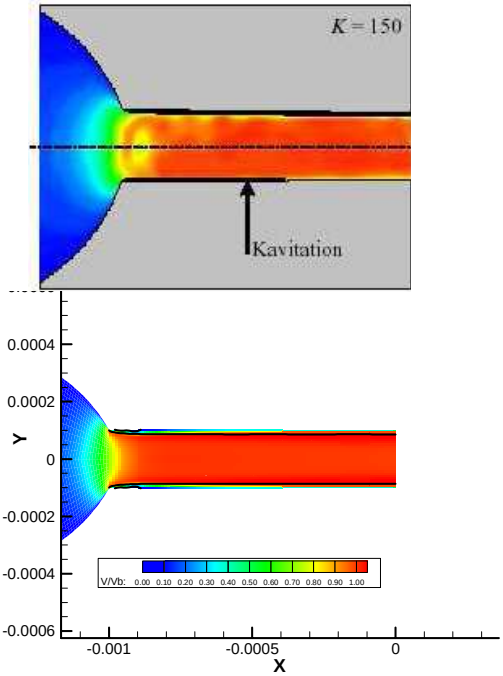

Figure 7: Velocity field/ Bernoulli velocity – Rc=10 µm- 15 MPa / 0.1 MPa comparaison EOLE/PIV measurements [6]

For this fully developed cavitation case, the velocity field is homogeneous in all the liquid part of the hole except at the entrance.

5

A comparison is done in figure 8 on the axial velocity profiles near the hole entrance at 50 µm and near the hole exit at 950 µm. The levels and the profiles of the axial velocities are correctly reproduced in both cases. As for the measurements, the velocity is close to the Bernoulli velocity on a large part of the hole exit (figure 9). This is due to the lateral spread of cavitation which is correctly reproduced. As J. Walther observed, no boundary layer develops along the cavitation sheets and this leads to a particularly homogeneous velocity profile, which we confirm.

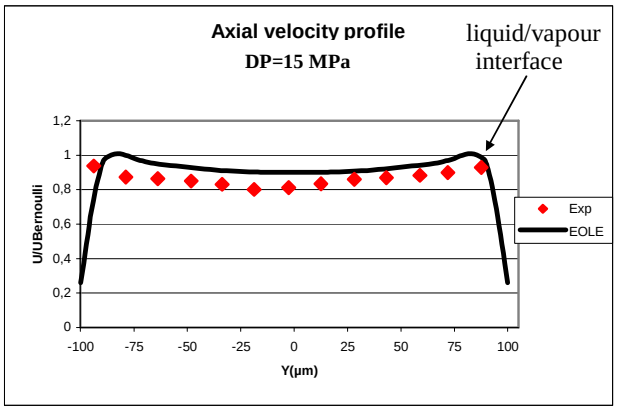

Figure 8: Comparison EOLE/PIV measurements [6] of the radial velocity profile in a section of the hole located at 50 µm from the hole inlet- Rc=10 µm – 15 MPa / 0.1 MPa

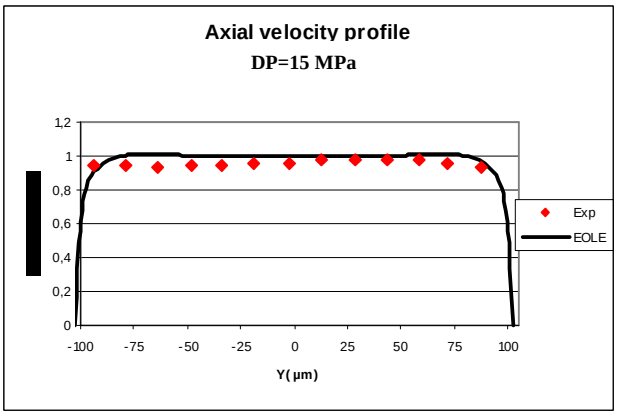

Figure 9: Comparison EOLE/PIV measurements [6] of the radial velocity profile in a section of the hole located at 950 µm from the hole inlet- Rc=10 µm – 15 MPa / 0.1 MPa

Unsymmetrical one hole injector with needle lift

The second example is issued from the PhD work of Saliba [10], [11] at Ecole Centrale de Lyon. This author has also used transparent nozzles with one axial hole, but with a moving needle. Various geometries of the hole were considered (cylindrical, convergent and divergent conical).

The geometric profiles of the sac and holes have been measured including the radii of curvature at the hole entrances. The needle lift was acquired and the sac pressure was measured in each case for a metallic nozzle having the same geometry as the transparent one. So the instantaneous cavitation number through the hole was evaluated during the needle lift. Injection pressures in the range 30 MPa –70 MPa were used with Diesel test oil. Measurements of the cavitation spread were done by shadowgraphy and tomography and correlations were also done with the spray break-up, having measured the microscopic spray angle. Thereafter the same measurements were applied to two hole transparent nozzles.

We chose to do comparisons on a nozzle having a cylindrical hole. Due to a delicate process of realization, this hole presents a small excentricity relatively to the sac of the nozzle.

The hole length is 1.79 mm and the hole diameter is 392 µm. The radii of curvature are different on the right and the left edges of the hole entrance (Rcr=26 µm, Rcl=51 µm). The operating condition is 30 MPa into 1 MPa. Some numerical results are presented at low needle lift (figure 10) and maximum lift (figure 11) and compared to the experimental results.

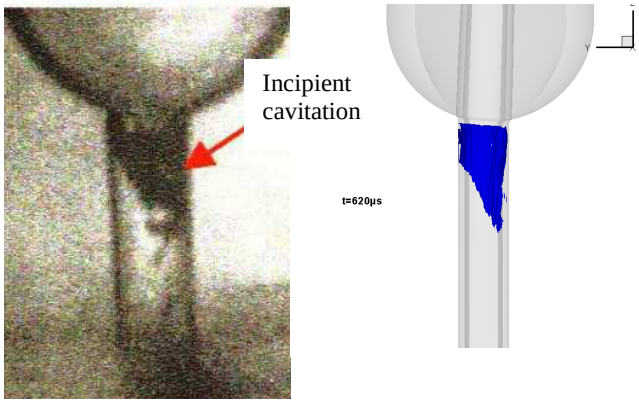

Figure 10: Incipient cavitation at low needle lift (10% opening)–comparison with measurements 30 MPa/1 MPa [10]

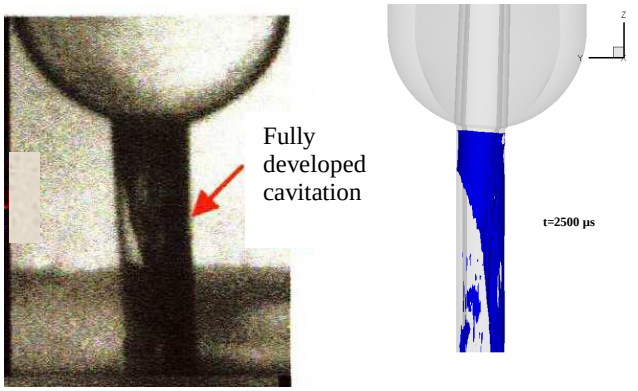

Figure 11: Fully developed cavitation at high needle lift (100% opening)-comparison with measurements 30MPa /1MPa [10]

6

The evolution of the cavitation with respect to the needle lift is correctly reproduced by the numerical model. Compared to the measurements, the numerical results show the same spread of cavitation as the needle opens. The unsymmetrical behaviour of the cavitation due to the excentricity of the needle is also put into evidence. Some instabilities of the flow rate appear due to the unsteadiness of the cavitation process.

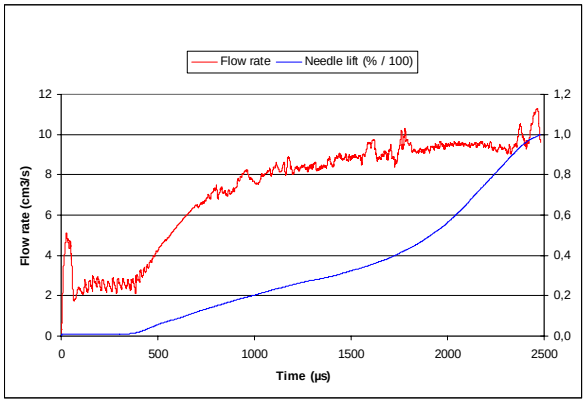

Figure 12: Evolution of the flow rate with the needle lift

DIESEL INJECTOR

A computation is now carried out on a symmetrical 6 holes Diesel injector (figure 13). Due to symmetry conditions, only 1/6 of the geometry is considered. The mesh is an O-type mesh comprising 160000 cells.

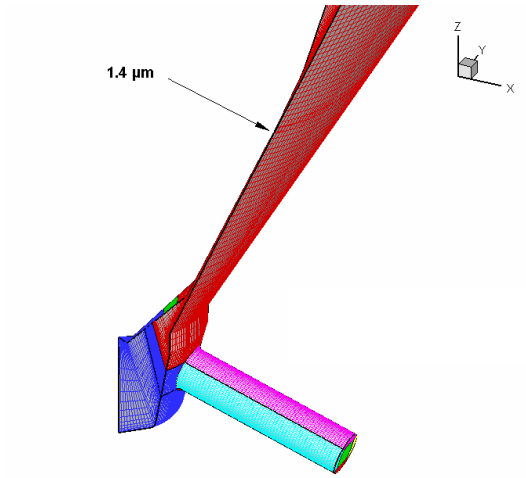

Figure 13: Multi-block mesh of the injector

The main geometrical characteristics of the injector are the following: the hole is cylindrical with a length equal to 0.6 mm and the hole diameter is 150 µm. The upper and lower radii of curvature of the hole inlet are known from prints performed on the nozzle. The injection pressure is 10.9 MPa into 8 Mpa. The minimum lift which has been calculated is 2 µm (1.4 µm orthogonally to the walls).

At low lift of the needle (figure 14), cavitation develops inside the needle seat and in the sac, due to constraints of the flow in this area where the pressure tends to drop strongly. This cavitation is convected from the sac to the hole as the needle is opening.

When the needle is opened enough (L>30%), the cavitation sheet which has formed remains fixed in the upper part of the hole entry. A fully developed cavitation regime is then issued highlighting some instabilities of the process, with shedded cavities emitted through break-up mechanisms of the main cavitation sheet.

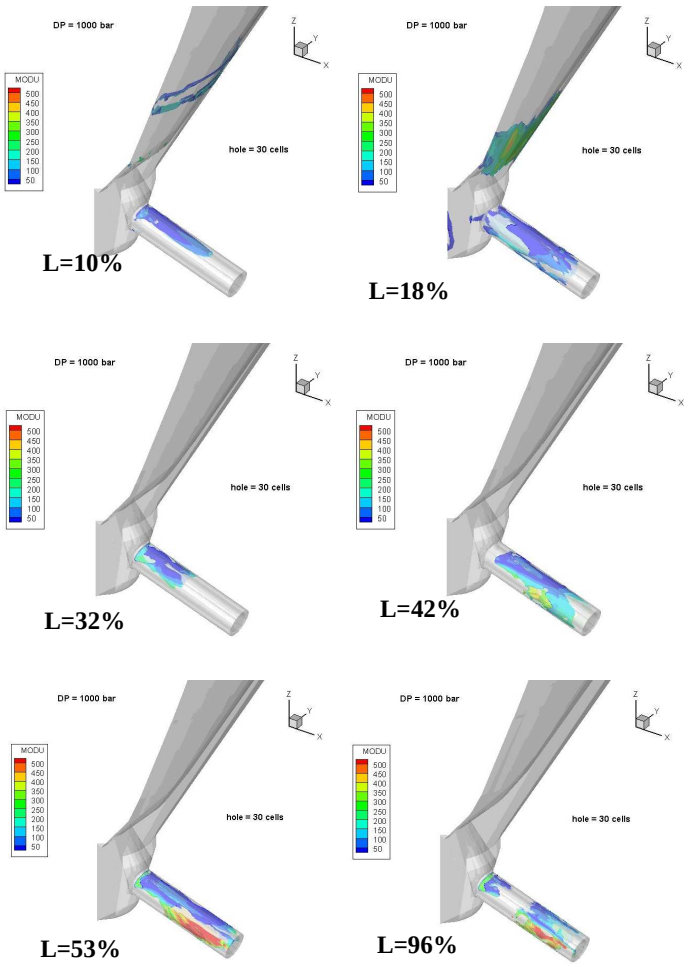

Fig 14: Evolution of the cavitation with the needle lift (expressed in % of the maximum lift) at 100 MPa / 0.1 MPa

The cavitation reaches a quasi-periodical behaviour as it can be seen on the flow rate evolution (figure 15), for a lift higher than 40% of the maximum lift (beyond t=60µs).

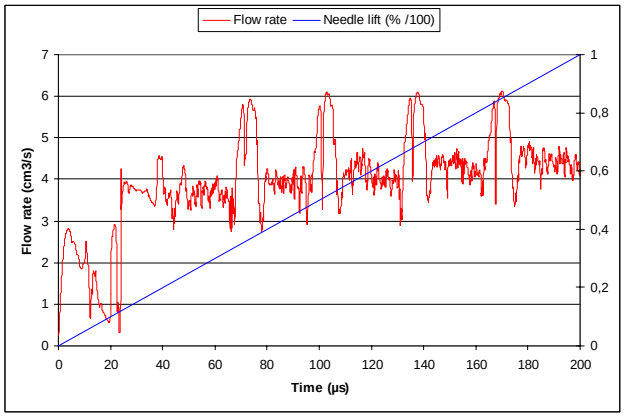

Figure 15: Evolution of the flow rate with the needle lift

7

CONCLUSION

In this paper, we have shown the ability of a VOF methodology including mass transfer to correctly reproduce cavitating flows in two simple and well documented configurations, in particular the spread of cavitation zones and the velocity profiles.

A new methodology has been set-up to handle the whole injection phase, especially for very low lifts (2 µm). We know that the correct value of the injection velocity (mean and turbulent) has as much importance as the flow rate value for doing correct combustion calculations with codes such as Fire, Kiva, Star-cd… This is particularly true in the transient phases of the needle lift, and validations have still to be systematically undertaken for these transient conditions. But improvements have also to be done in order to take into account the effects of wall roughness along the needle, particularly at very low lifts, and along the holes.

ACKNOWLEDGMENTS

The authors would like to thank particularly on one hand J. Walther and Pr. C. Tropea at Technische Universität Darmstadt, on the other hand R. Saliba and Pr. Champoussin at Ecole Centrale de Lyon for the use of their experiments as validation data for the code Eole. The PhD work of J. Walther has been undertaken under Bosch support which is also gratefully acknowledged. P. Gastaldi at Renault is thanked for having allowed to publish these results.

REFERENCES

[1] Busch: "Untersuchung von Kavitationsphänomenen in Dieseleinspritzdüsen" Dissertation, Hannover 2001

[2] Chaves, Knapp, Kubitzek, Obermeier and Schneider: "Experimental study of cavitation in the nozzle hole of Diesel Injectors using transparent nozzles", SAE 950290

[3] Roth, Gavaises and Arcoumanis: "Cavitation initiation, its development and link with flow turbulence in Diesel injector nozzles", SAE 2002-01-0214

[4] Winklhofer, Kull, Kelz, Morozov: "Comprehensive hydraulic and flow field documentation in model throttle experiments under cavitation conditions", ILASS-Europe Zürich 2-6/09/2001

[5] Collicott, Li: "True-scale true pressure internal flow visualization for Diesel injectors": SAE 2006-01-0890

[6] Walther: "Quantitative Untersuchungen der Innenströmung in kavitierenden Dieseleinspritzdüsen", Dissertation, TU Darmstadt 2002

[7] Badock: "Untersuchungen zum Einfluss der Kavitation auf den primären Strahlzerfall bei der dieselmotorischen Einspritzung", Dissertation, Darmstadt 1999.

[8] Arcoumanis, Badami, Flora and Gavaises: "Cavitation in real-size multi-hole Diesel injector nozzles", SAE 2000-01-1249

[9] Miranda, Chaves, Martin and Obermeier: "Cavitation in a transparent real size VCO injection nozzle", ICLASS 2003, Sorento.

[10] Saliba: "Investigations expérimentales sur les phénomènes de cavitation et d'atomisation dans les injecteurs Diesel" Thèse Ecole Centrale de Lyon 2006

[11] Saliba: "Cavitation effect on the near nozzle spray development in high pressure Diesel injection", ILASS meeting, Nottingham 09/2004.

[12] Soteriou, Andrews and Smith:"Direct injection Diesel sprays and the effect of cavitation and hydraulic flip on atomization", SAE 950080.

[13] Payri, Guardiola, Salvador, Gimeno: "Critical cavitation number determination in Diesel injection nozzles", Experimental Techniques n° 49, 2004

[14] Chaves, Ludwig: "Characterization of cavitation in transparent nozzles depending on the nozzle geometry", ILASS-Europe, Nottingham 2004.

[15] Giannadakis, Papoulias, Gavaises, Arcoumanis, Soteriou and Tang: "Evaluation of the predictive capability of Diesel nozzle cavitation models", SAE 2007-01-0245

[16] Kubo M, Araki and Kimura (2003): "Internal flow analysis of nozzles for DI Diesel engines using a cavitation model", J.S.A Review 24, pages 255, 261.

[17] Schmidt, Rutland and Corradini (1997): "A numerical study of cavitating flow through various nozzle shapes", SAE 971597.

[18] Schmidt and Corradini (1997): "Analytical prediction of the exit flow of cavitating orifices", Atomization and Sprays, vol. 7, pp. 603-616.

[19] Habchi, Dumont and Simonin (2003): "Cavif: a 3D code for the modelling of cavitating flows in Diesel injectors", ICLASS, Sorrento, july 2003.

[20] Xu, Bunnell and Heister (2001): "On the influence of internal flow structure on performance of plain-orifice atomizers", Atomization and sprays, vol. 11, pp 335-350.

[21] Tatschl, Künsberg Sarre, Alajbegovic and Winklhofer (2000): "Diesel spray break-up modelling including multidimensional cavitating nozzle flow effects", ILASS Darmstadt, september 2000.

[22] Cokljat, Ivanov and Vasquez (1998): "Two-phase model for cavitating flows", 3rd Int. Conference on multiphase flows, ICMF'98, Lyon.

[23] Marcer, Le Cottier, Chaves, Argueyrolles, Habchi and Barbeau (2000): "A validated numerical simulation of Diesel injector flow using a VOF method", SAE Paper 2000-01-2932.

[24] Marcer, Le Gouez (2001): " Simulation of unsteady cavitating flows in Diesel injector with an improved VOF method", ILASS Zürich, september 2001.

[25] Marcer "Further validation of the EOLE code for Diesel direct injection modelling", 20th ILASS Europe, Orléans, Sept. 2005.

[26] Marcer: "A CFD code for Diesel Direct Injection Simulation", ICLASS 2003, 9th Conference on Liquid Atomization & Spray Systems, Sorrento, July 2003.

[27] De Jouëtte, Viviand, Wornom, Le Gouez (1991): "Pseudo-compressibility method for incompressible flow calculation", 4th Int. Symposium on Comp. Fluid Dyn. of California at Davis, sept 9-12 1991

[28] Biausser, Guignard, Marcer, Fraunié (2004): "3D two phase flows numerical simulations by SL-VOF method", Int. J. Num.. Meth. Fluids, 45:581-604.